

PHYSICAL REVIEW C

NUCLEAR PHYSICS

THIRD SERIES, VOLUME 49, NUMBER 4

APRIL 1994

RAPID COMMUNICATIONS

The Rapid Communications section is intended for the accelerated publication of important new results. Manuscripts submitted to this section are given priority in handling in the editorial office and in production. A Rapid Communication in Physical Review C may be no longer than five printed pages and must be accompanied by an abstract. Page proofs are sent to authors.

Excitation energy deposition in central collisions of 40A MeV ^{40}Ar with ^{232}Th

D. Utley, R. Wada, K. Hagel, J. Li, X. Bin, M. Gui, Y. Lou, R. Tezkratt,* J. B. Natowitz, and M. Gonin†
Cyclotron Institute, Texas A & M University, College Station, Texas 77843

(Received 8 December 1993)

Excitation energy depositions in the reactions of 40A MeV ^{40}Ar with ^{232}Th have been determined from measurements of neutron multiplicities in coincidence with mass identified heavy reaction products. For the most central collisions the derived excitation energies of 880 MeV are 200–300 MeV above previous estimates and in excellent agreement with momentum transfer systematics. Heavy evaporation residues are observed for these collisions indicating apparent dynamic delays in the fission channel of $(1-5)\times 10^{-20}$ s. While a massive-transfer simulation incorporating pre-equilibrium emission is in generally good agreement with the experimental results evidence is also found for strongly damped collisions.

PACS number(s): 25.70.Jj, 25.70.Lm, 25.85.Ge

Defining the dominant reaction mechanisms, the excitation energy depositions and the subsequent decay modes for very highly excited nuclei has been the goal of a significant fraction of recent heavy ion reaction studies [1–8]. A system of particular interest has been $^{40}\text{Ar} + ^{232}\text{Th}$ at energies of (30–77)A MeV. The $^{40}\text{Ar} + ^{232}\text{Th}$ system has been extensively studied since early measurements of Conjeaud *et al.* [2] indicated that the most central collisions did not appear to lead to binary fission, making this system a potentially good candidate for studies of multifragmentation [9,10]. Subsequent neutron ball experiments designed to probe the excitation energy deposition in those reactions led to a suggestion of “soft saturation” in the excitation energy deposition with increasing energy [6]. That work and more recent extensions of that work [7,8] have been interpreted as providing evidence that linear momentum transfer systematics derived from low energy measurements [11,12] and the massive-transfer and preequilibrium scenarios often employed to model such transfers [13–17] are seriously inadequate. At the same time, a recent phenomenologi-

cal model based on those ingredients has been shown to model the basic trends reported in the inclusive data [17]. Interestingly, a model based entirely on the assumption of deep inelastic collisions also reproduces the observed neutron spectra in a reasonable fashion [18], indicating that more detailed experiments are required to provide an unambiguous interpretation of the data.

In this work we present results of experiments for 40A MeV $^{40}\text{Ar} + ^{232}\text{Th}$ in which collisions leading to excitation energies significantly above those derived from previous measurements of neutron multiplicities have been observed. The signature products of those collisions are the highest velocity heavy residues and fission fragments observed at very small laboratory angles, $\theta_L = 3^\circ-9^\circ$. An initial compound nucleus of $A \approx 260$ with an excitation energy of 880 MeV is inferred from our results. This result is consistent with linear momentum transfer systematics. The survival of evaporation residues from such very excited heavy compound nuclei apparently reflects the fact that the times required for fission are much longer than for particle emission. The effects of such a fission delay can be seen in the product mass distribution and in the variation of neutron multiplicity with heavy product mass.

Experiments were completed with 40A MeV Ar^{14+} beams supplied by the Texas A & M University K500 superconducting cyclotron. All experiments were carried

* Also at Department of Physics and Astronomy, Vanderbilt University, Nashville, TN 37235.

† Also at Department of Physics, Brookhaven National Laboratory, Upton, NY 11973.

out in the reaction chamber of the neutron ball [19]. The ball is an 1800 liter tank of pseudocumene loaded with Gd (0.3% by wt). Light produced either by energy loss of recoiling protons or of gamma rays produced following neutron capture by Gd (or H) is detected by eighteen photomultiplier tubes during a 100 μ s counting period. To reduce the background a twofold coincidence is required for the photomultiplier signals.

Background measurements were made during the experiments by opening a second gate following the trigger gate. Background corrections were made by subtracting the average background values from the average multiplicity of detected neutrons. The multiplicity values reported are corrected for a 3% bleed over into the background gate from the first gate. The Th target was ThF₄, 315 μ g/cm², on a 50 μ g/cm² C backing.

To allow detection of forward directed reaction products, the neutron ball vacuum chamber has a forward extension. For the mass measurements a microchannel plate timing detector was used with a 900 mm² silicon detector. The flight path between these detectors was 125 cm. This time-of-flight arm was at $\theta_L = 6^\circ$. The flight time information combined with the energy signals from the silicon detector allowed calculation of the mass of the detected particle during the analysis. The overall time resolution was 1 ns.

Energy calibrations were made using alpha sources from ²⁵²Cf (6.11 MeV), ²⁴¹Am (5.48 MeV), and ¹⁴⁸Gd (3.18 MeV). Linearity was checked using a precision pulse generator and decade attenuator. Pulse height defects for heavy fragments and residues were determined using Cf fission sources and scattered and degraded beams of 2A MeV ¹⁸¹Ta using the formulation of Kaufman *et al.* [20]. Timing calibrations were made using delay lines in the timing circuits. Plasma delays were determined from the measured times and the known timing from the scattered reference beam.

To determine the neutron detection efficiencies in our experiment we have used the EUGENE code [17] to simulate the reaction kinematics. We have then used the laboratory frame events generated by this code together with measured ²⁵²Cf neutron efficiencies and simulations of the neutron ball efficiency which includes both geometry and neutron interaction cross sections as a function of neutron energy to determine the overall neutron efficiency. This efficiency includes contributions from all sources including preequilibrium emission and evaporation from both projectilelike and targetlike sources. In spite of the model dependence, we believe this to be more accurate than assuming that all detected neutrons are of evaporation origin.

Initial neutron ball calibrations were made using neutrons from ²⁵²Cf sources triggered by fission fragments detected in silicon strip detectors. The neutron ball response function was determined using the code DENIS-V [21] as modified by B. Hurst [22]. The net efficiencies used for the final analysis were calculated using the ²⁵²Cf measurement as a reference. The net efficiency used in the analysis also incorporates the effect of the emission of the neutrons from a moving source. Neutrons from a forward moving source have an enhanced probability of

escaping from the neutron ball prior to thermalization and capture. For example, for 40A MeV ⁴⁰Ar on ²³²Th, as modeled with the code EUGENE [17] and an efficiency of 69.8% for ²⁵²Cf neutrons, the neutron efficiency for an event with 15 emitted neutrons is 57% and the efficiency for an event resulting in the emission of 45 neutrons drops to 53%. The fraction of total neutrons lost through the forward time-of-flight wedge in the neutron ball is 11% while 23% of the neutrons emitted in a preequilibrium source are lost. These numbers clearly reveal that source dynamic characteristics must be incorporated in the analysis. Data analysis was completed off-line using the code LISA [23].

The product laboratory velocity reveals the degree of interaction of the target and projectile. Figure 1 presents a plot of velocity versus mass for the products detected at $\theta_L = 6^\circ$. The velocities are truncated at 6 cm/ns since higher velocity lighter particles were not stopped in the Si detector.

In the plot a high count rate region is seen for products with $A \leq 40$. Such products include projectilelike fragments and intermediate mass fragments, as well as, light evaporated particles. A group of fragments with relatively high probability is seen near 4 cm/ns. These velocities are strongly damped relative to the beam velocity of 8.8 cm/ns. Above mass 40 a narrow band of prod-

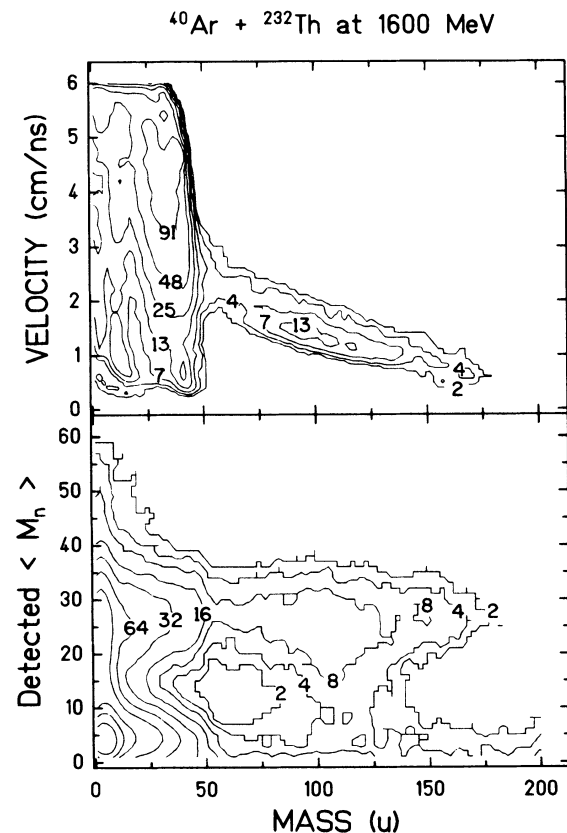


FIG. 1. Product velocity and neutron multiplicity as a function of product mass at $\theta_L = 6^\circ$. (a) Product velocity vs mass; (b) raw neutron multiplicity (not corrected for efficiency or background) vs mass. The efficiency for ²⁵²Cf neutrons is 78.6%. The contour levels are indicated.

ucts is seen extending to $A \approx 180$. For this group the average velocity decreases monotonically with increasing mass. A region of relatively high product intensity centered near $A \approx 100$ is identified as fission fragments. Beyond this fission fragment peak and extending up to $A \approx 185$ is a group of products having average velocities of 0.5 to 1 cm/ns which we tentatively identify as evaporation residues.

In Fig. 1(b) the raw (uncorrected for background) neutron multiplicities are plotted against mass. In this figure, the most prominent feature is a band of high multiplicity near 25 neutrons which extends across the entire mass region indicating that relatively high excitation energies are associated with products in each region. For most of the mass range the neutron multiplicity distributions are bimodal, having another peak at low neutron multiplicity.

To further delineate the neutron multiplicity we focus on the higher multiplicity band in the neutron distribution and plot the background corrected average multiplicities against mass in Fig. 2(a), for projectilelike fragments having velocities near the beam velocity (measured in a separate experiment and not shown in Fig. 1), for fragments with $A < 40$ and velocities near 4 cm/ns [corresponding to the group of products coming from strongly damped collisions which are noted in Fig. 1(a)] and for heavy products with $A > 40$. For the projectilelike frag-

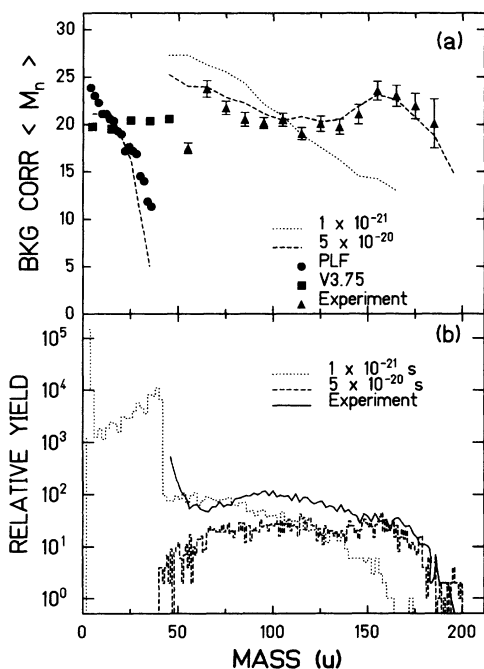


FIG. 2. Background corrected average neutron multiplicity and relative yield as a function of product mass at $\theta_L = 6^\circ$. (a) $\langle M_n \rangle$ vs mass. The solid points represent experimental data. The dotted line represents the results of a EUGENE calculation with 1×10^{-21} s fission delay. The dashed line represents the calculation with 5×10^{-20} s fission delay. For projectilelike fragments the two calculations are identical; (b) yield vs mass. The solid line represents the data. The dotted and dashed lines represent results of the EUGENE calculation as in part (a).

ments we note that as the mass decreases, the neutron multiplicity increases. This behavior has been reported often and is characteristic of massive-transfer reactions [13,14,17]. The strongly damped products with $V_L \approx 4$ cm/ns appear to be products of relaxed events and are either evaporated or emitted in deep inelastic processes. The observed neutron multiplicities are very similar for this group of products independent of mass. The products with $A > 40$ show an interesting variation in neutron multiplicity peaking near 23.5 detected neutrons at $A = 65$ and again at $A = 155$ and reading below 20 neutrons at $A = 115$ and again at $A = 185$.

The observed trend with mass indicates that the lighter products in the fission group and the lighter products in the residue group both come from higher excitation energies than the heavier products in each group. We take these products as representative of the central collisions where preequilibrium emission determines the limits to excitation energy. The observed increase in detected neutron multiplicity for the lighter products in each group translates to nearly twice that amount when efficiency corrected. That in turn represents a large difference in excitation energy as can be seen in Fig. 3 where we have plotted the total neutron multiplicity as a function of deposited excitation energy as calculated by the phenomenological event generator EUGENE [17] and by a hybrid version using the entrance channel dynamics of the code EUGENE, but using the code GEMINI [24] to follow the subsequent statistical deexcitation cascade.

As seen in Fig. 3 when the excitation energy increases the rate of increase of neutron multiplicity with excitation energy decreases, reflecting increasing competition from charged particle emission. At higher energies, the rate is of the order of 1 emitted neutron/60 MeV excitation energy. Results are essentially the same from the two calculations.

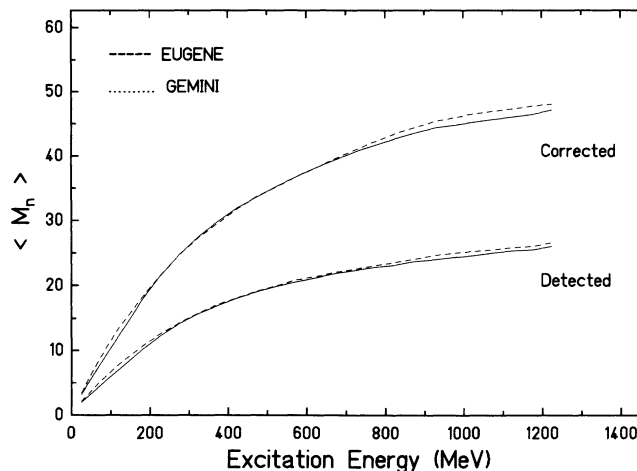


FIG. 3. Model calculations of neutron multiplicity as a function of deposited excitation energy. The primary multiplicity from all sources resulting from two calculations using the code EUGENE and a hybrid code EUGENE GEMINI as discussed in text are presented. Predicted values for detected $\langle M_n \rangle$ are obtained by filtering the calculation with the detector geometry and intrinsic efficiency. An efficiency of 69.8% for ^{252}Cf neutrons was used in this calculation.

TABLE I. Experimentally derived excitation energies for most central collisions of 40A MeV Ar with ^{232}Th and for $A \geq 40$ products detected at $\theta_L = 6^\circ$.

A	$\langle \text{det}M_n \rangle^a$	$\langle M_n \rangle^b$	E_x (MeV)
155	23.5 ± 1.0	44 ± 2	870^{+120}_{-110}
65	23.7 ± 0.9	44 ± 2	890^{+110}_{-100}
$40 \leq A \leq 185$	19.1 ± 0.6	33.8 ± 1.1	480^{+40}_{-30}

^aCf-252 neutron efficiency 69.8%.

^bEfficiency corrected neutrons. Includes response function of the neutron ball.

In Table I we present the observed and efficiency corrected neutron multiplicities derived from our work for the two maxima observed for the heavy products in Fig. 2(a). Using the derived primary multiplicities we determined primary excitation energies by comparing the primary neutron multiplicities with the calculated curve of Fig. 3. For the highest average neutron multiplicity of 44 ± 2 the excitation energies presented in Table I are in good agreement with excitation energies derived from linear momentum transfer systematics assuming a limit near 180 MeV/c [11,12] as well as with preequilibrium calculations [2,15,16] and are 200–300 MeV higher than results previously obtained from most probable neutron multiplicity measurements [6–8]. Those previous results, cross section weighted over a wide range of impact parameters and momentum transfers, are not representative of the most central collisions and in fact are more akin to the total heavy fragment results in Table I. The average multiplicity of 34 neutrons associated with heavy products, with $40 \leq A \leq 185$ reported in Table I, is in reasonable agreement with values recently derived from most probable neutron numbers [8].

Given the good agreement it is of interest to ask how the EUGENE results filtered for our fragment detection efficiency compare with the experimental data. In Fig. 2 we present results for a calculation with no dynamic delay and for a fission delay time of 5×10^{-20} s [25] [we find similar results for $(1 \text{ to } 5) \times 10^{-20}$ s delays]. We note that for both projectilelike and heavy products the massive-transfer preequilibrium scenario appears to work very well if the dynamic fission delay is included. At the same time, the group of relaxed deep inelastic products

seen in our work are not seen in the results of this reaction simulation which does not include strong dissipation. It is interesting to note that those strongly damped products have neutron multiplicities equal to those seen for the bulk of the fission fragments and thus appear to be of similar origin. This may account for the larger yield of fission fragments relative to residues seen in the experiment when compared to the model calculations in Fig. 2(b). The deep inelastic collisions probably occur at intermediate impact parameters, perhaps in direct competition with massive transfer [26–28]. They may also be responsible for the heavier products seen at wider angles by Schwinn *et al.*, but reported to have neutron multiplicities like those of the bulk products [7].

In conclusion our results indicate that the products of the most central collisions of 40A MeV ^{40}Ar with ^{232}Th are the light fission fragments and evaporation residues. The excitation energies associated with these products are 880 ± 120 MeV, in good agreement with linear momentum transfer systematics. The survival of the evaporation residues for highly excited compound nuclei is in accord with other recent observations [29,30] and predictions [31,32] and appears to reflect dynamic delays in the fission process of $(1-5) \times 10^{-20}$ s. Such delays allow the highest excitation energy nuclei to survive fission but are insufficient to allow products of intermediate excitation energy (arising from intermediate impact parameters) to escape fissioning. It is neutrons from these latter relatively high cross section collisions which dominate the inclusive neutron distributions and determine the most probable neutron numbers previously reported [6–8]. A massive-transfer plus preequilibrium picture such as that incorporated in the code EUGENE [17] provides a reasonable picture of many aspects of the collision when fission delay is included, but cannot account for very damped products which appear to result from the same range of intermediate excitation energies as the bulk of the fission fragments.

We thank D. Durand for making the code EUGENE available to us. We also appreciate the efforts of the technical staff of the TAMU Cyclotron Institute. This work was supported by the United States Department of Energy under Grant No. DE-FG05-86ER40256 and by the Robert A. Welch Foundation.

[1] *Proceedings of the Fourth International Conference on Nucleus-Nucleus Collisions*, edited by H. Toki, I. Tanihata, and H. Kamitsubo [Nucl. Phys. **A538** (1992)].
[2] M. Conjeaud, S. Harar, M. Mostefai, E. C. Pollacco, C. Volant, Y. Cassagnou, R. Dayras, R. LeGrain, H. Oeschler, and F. Saint-Laurent, Phys. Lett. **159B**, 244 (1985).
[3] G. Bizard, R. Bougault, R. Brou, J. Colin, D. Durand, A. Genoux-Lubain, J. L. Laville, C. Le Brun, J. F. Lecolley, M. Louvel, J. Peter, J. C. Steckmeyer, B. Tamain, A. Badala, T. Motobayashi, G. Rudolf, and L. Stuttge, Phys. Lett. B **302**, 162 (1993).
[4] B. Borderie, Ann. Phys. (Fr.) **17**, 349 (1992).

[5] G. Bizard, R. Brou, P. Eudes, J. L. Laville, J. Natowitz, J. P. Patry, J. C. Steckmeyer, B. Tamain, A. Thiphagne, H. Doubre, A. Peghaire, J. Peter, E. Rosato, J. C. Adloff, A. Kamili, G. Rudolf, F. Scheibling, F. Guilbault, C. Le Brun, and F. Hanappe, *Proceedings of the Texas A&M Symposium on Hot Nuclei*, edited by S. Shlomo, R. P. Schmitt, and J. B. Natowitz (World Scientific, Singapore, 1988), p. 262.
[6] D. X. Jiang, H. Doubre, J. Galin, D. Guerreau, E. Piasecki, J. Pouthas, A. Sokolov, B. Cramer, G. Ingold, U. Jahnke, E. Schwinn, J. L. Charvet, J. Frehaut, B. Lott, C. Magnago, M. Morjean, Y. Patin, Y. Pranal, J. L. Uzureau, B. Gatty, and D. Jacquet, Nucl. Phys. **A503**,

- 560 (1989).
- [7] E. Schwinn, U. Jahnke, J. L. Charvet, B. Cramer, H. Doubre, J. Frehaut, J. Galin, B. Gatty, D. Guerreau, G. Ingold, D. Jacquet, D. X. Jiang, B. Lott, M. Morjean, C. Magnago, Y. Patin, J. Pouthas, E. Piasecki, and A. Sokolov, submitted to *Z. Phys.*
- [8] B. Lott, J. L. Charvet, E. Crema, G. Duchene, H. Doubre, J. Frehaut, J. Galin, B. Gatty, D. Guerreau, G. Ingold, D. Jacquet, U. Jahnke, D. X. Jiang, C. Magnago, M. Morjean, Y. Patin, E. Piasecki, J. Pouthas, Y. Pranal, F. Saint-Laurent, E. Schwinn, A. Sokolov, J. L. Uzureau, and X. M. Wang, *Z. Phys. A* **346**, 201 (1993).
- [9] J. B. Natowitz, *Nuclear Dynamics and Nuclear Disassembly* (World Scientific, Singapore, 1989).
- [10] D. R. Bowman, C. M. Mader, G. F. Peaslee, W. Bauer, N. Carlin, R. T. de Souza, C. K. Gelbke, W. G. Gong, Y. D. Kim, M. A. Lisa, W. G. Lynch, L. Phair, M. B. Tsang, C. Williams, N. Colonna, K. Hanold, M. A. McMahan, G. J. Wozniak, L. G. Moretto, and W. A. Friedman, *Phys. Rev. C* **46**, 1834 (1992).
- [11] V. E. Viola, B. B. Back, K. L. Wolf, T. C. Awes, C. K. Gelbke, and H. Breuer, *Phys. Rev. C* **26**, 178 (1982).
- [12] S. Leray, *J. Phys. C* **4**, 275 (1986).
- [13] J. Wilczynski, K. Siwek-Wilczynska, J. Van Driel, S. Gonggrijp, C. J. M. Hageman, R. V. F. Janssens, J. Lukasiak, R. H. Siemssen, and Y. Van der Werf, *Nucl. Phys. A* **373**, 109 (1982).
- [14] B. G. Harvey and M. J. Murray, *Phys. Lett.* **130B**, 373 (1983); B. G. Harvey, *Nucl. Phys. A* **444**, 498 (1985).
- [15] M. Blann, *Phys. Rev. C* **31**, 1245 (1985).
- [16] J. B. Natowitz, S. Leray, R. Lucas, C. Ngo, E. Tomasi, and C. Volant, *Z. Phys. A* **325**, 467 (1986).
- [17] D. Durand, *Nucl. Phys. A* **541**, 266 (1992).
- [18] H. W. Barz, J. P. Bondorf, C. H. Dasso, R. Donangelo, G. Pollarolo, H. Schulz, and K. Sneppen, *Phys. Rev. C* **46**, 42 (1993).
- [19] R. P. Schmitt, *Proceedings of the International Conference on New Nuclear Physics with Advanced Techniques* (World Scientific, Singapore, 1992), p. 182.
- [20] S. Kaufman, E. Steinberg, B. Wilkins, J. Unik, A. Gorski, and M. Fluss, *Nucl. Instrum. Methods* **115**, 47 (1974).
- [21] J. Poitou and C. Signarbieux, *Nucl. Instrum. Methods* **114**, 113 (1974).
- [22] B. Hurst, Ph.D. thesis, Texas A&M University, 1994, in preparation.
- [23] W. Kuhn and B. Kolb, private communication.
- [24] R. J. Charity, M. A. McMahan, G. J. Wozniak, R. J. McDonald, L. G. Moretto, D. G. Sarantities, L. G. Sobotka, G. Guarino, A. Pantaleo, L. Fiore, A. Gobbi, and K. D. Hildenbrand, *Nucl. Phys. A* **483**, 371 (1988).
- [25] D. Hilscher and H. Rossner, *Ann. Phys. (Fr.)* **17**, 471 (1992).
- [26] M. Rivet, B. Borderie, P. Box, M. Dakowski, C. Cabot, D. Gardes, D. Jouan, G. Mamane, X. Tarrago, H. Utsunomiya, Y. El Masri, F. Hanappe, F. Seville, and F. Haddad, IPN Orsay Report No. IPNO-DRE-93-12, 1993 (unpublished).
- [27] B. Lott, S. P. Baldwin, B. M. Szabo, B. M. Quednau, W. U. Schroeder, J. Toke, L. G. Sobotka, J. Barreto, R. J. Charity, L. Gallamore, D. G. Sarantities, D. W. Stracener and R. T. de Souza, *Phys. Rev. Lett.* **68**, 3141 (1992).
- [28] R. Wada, K. Hagel, R. Tezkratt, G. X. Dai, S. Lee, J. Blackadar, Y. Lou, D. Utley, B. Xiao, J. Li, N. Mdeiwah and J. B. Natowitz, in preparation.
- [29] S. Beiersdorf, R. A. Esterlund, M. Knaack, W. Westmeier, P. Patzelt, F. P. Hessberger, V. Ninov, and A. Luttgen, *Phys. Lett. B* **286**, 225 (1992).
- [30] F. P. Hessberger, V. Ninov, and D. Ackermann, *Z. Phys. A* **343**, 301 (1992).
- [31] M. Gonin, L. Cooke, B. Fornal, P. Gonthier, M. Gui, Y. Lou, J. B. Natowitz, G. Nardelli, G. Nebbia, G. Prete, R. P. Schmitt, B. Srivastava, W. Turmel, D. Utley, H. Utsunomiya, G. Viesti, R. Wada, B. Wilkins, and R. Zanon, *Nucl. Phys. A* **495**, 139 (1989).
- [32] P. Frobich, I. I. Gontchar, and N. D. Mavlitov, *Nucl. Phys. A* **556**, 281 (1993).